Journal of The Electrochemical Society, 2021 **168** 046505

Electrodeposition of Tungsten from Molten KF–KCl–WO_3 and CsF–CsCl–WO_3

Toshiyuki Nohira,[1,*,z] Tatsuya Ide,[1] Xianduo Meng,[1] Yutaro Norikawa,[1] and Kouji Yasuda[2,3,*,a]

[1]*Institute of Advanced Energy, Kyoto University, Gokasho, Uji 611-0011, Japan*
[2]*Graduate School of Energy Science, Kyoto University, Yoshida-honmachi, Sakyo-ku, Kyoto 606-8501, Japan*
[3]*Agency for Health, Safety and Environment, Kyoto University, Yoshida-honmachi, Sakyo-ku, Kyoto 606-8501, Japan*

Electrodeposition of W coatings in KF–KCl eutectic melts was investigated after adding 0.5–2.0 mol% of WO_3 at 923 K. Cyclic voltammetry at a Ag electrode suggested that the electrodeposition of W from W(VI) ions proceeds from 1.65 V vs K^+/K. Electrodeposition of the α-W phase was confirmed by X-ray diffractometry (XRD). The effects of current density and amount of WO_3 on the morphology of W coatings were investigated by surface and cross-sectional scanning electron microscopy (SEM). The smoothest W coating with a thickness of ~15 μm was formed at 12.5 mA cm^{-2} and 2.0 mol% WO_3 in KF–KCl eutectic melts. By increasing the charge density, a coating thickness of ~30 μm was attained; however, it significantly increased the surface roughness of the coating. The electrodeposition of W was also performed in CsF–CsCl eutectic melts at a lower temperature of 873 K to suppress the growth of crystal grains. XRD confirmed the existence of both α-W and β-W phases in the W coatings deposited in the CsF–CsCl eutectic melts. SEM analyses revealed the successful formation of dense and smooth W coatings with ~30 μm thickness in the CsF–CsCl eutectic melts.

 [DOI: 10.1149/1945-7111/abf266]

Manuscript submitted January 13, 2021; revised manuscript received March 13, 2021. Published April 7, 2021. *This was paper 2988 presented during PRiME 2020, October 4–9, 2020. This paper is part of the JES Focus Issue on Molten Salts and Ionic Liquids II.*

Tungsten metal is known for its robustness, especially considering its high melting and boiling points and hardness. However, its hardness and brittleness make it difficult to work. Thus, the electrodeposition of flat and dense tungsten coatings is worth investigating. Numerous studies have reported the electrodeposition of tungsten from the high-temperature molten salts, such as fluorides,[1,2] chlorides,[2–4] fluoride–chloride mixtures[2–8] and oxides.[2,3,9] It is known that dense and coherent tungsten deposits are more easily obtained from molten fluorides than from molten chlorides. One drawback of typical fluoride melts such as LiF–NaF–KF is the difficulty in removing the adhered molten salts by water washing because of the limited solubilities of LiF and NaF in water.[10] Although good tungsten deposits can be electrodeposited from molten oxides,[9] the operation temperature tends to be very high, typically over 1123 K.

Recently, we successfully employed molten KF–KCl eutectic salt (T_{eu} = 878 K) as electrolyte baths for the electrodeposition of crystalline Si coatings[11] and Ti coatings.[12–14] Since all the component salts of KF and KCl are highly soluble in water,[10] the solidified salts on deposited coatings can be easily removed by water washing. So far, we have succeeded in obtaining crystalline Si coatings from the molten KF–KCl–K_2SiF_6 at 923 K[11] and smooth Ti coatings from the KF–KCl–K_3TiF_6 at 923 K.[12–14]

In the present paper, based on our previous studies, we demonstrated the use of KF–KCl molten salt for the electrodeposition of W coatings. WO_3 was employed as a tungsten source because it is easy to handle than gaseous WF_6. We investigated the effect of the W(VI) ion concentration and current density on the morphology of W coatings at 923 K. Further, the electrodeposition of W coatings was investigated in molten CsF–CsCl–WO_3 at 873 K. We have chosen molten CsF–CsCl eutectic salt (T_{eu} = 713 K) as a lower temperature molten salt to suppress the growth of crystal grains. The components of CsF and CsCl salts have even larger solubilities in water than those of KF and KCl salts.[10]

Experimental

For molten KF–KCl, the reagent-grades of KF (FUJIFILM Wako Pure Chemical Corp., > 99.0%) and KCl (FUJIFILM Wako Pure Chemical Corp., >99.5%) were mixed in the eutectic composition (molar ratio of KF:KCl = 45:55, melting point = 878 K, 400 g) and loaded in a graphite crucible (Toyo Tanso Co., Ltd.; o.d. 100 mm × i.d. 90 mm × height 120 mm). The mixture was successively dried under vacuum at 453 K for over 72 h and at 773 K for 24 h. Similarly, the molten CsF–CsCl was prepared by mixing the reagent-grades of CsF (Furuuchi Chemical Corp., >99.0%) and CsCl (FUJIFILM Wako Pure Chemical Corp., >99.0%) in the eutectic composition (molar ratio of CsF:CsCl = 50:50, melting point = 713 K, 500 g) and loaded in a graphite crucible. The mixture was initially dried under vacuum at 453 K for over 72 h and then under vacuum at 673 K for 24 h. The crucible with the mixture (KF:KCl or CsF:CsCl) was placed at the bottom of a stainless steel vessel in an airtight Kanthal container. The electrochemical measurements were conducted in a dry Ar atmosphere.

For Raman spectroscopy, small portions of KF–KCl and KF–KCl–WO_3 melts were sampled using a borosilicate glass tube (Pyrex®, o.d. 6 mm × i.d. 4 mm). The sampled salt was loaded into a Pt pan (Rigaku Corp., o.d. 5 mm × height 2.5 mm) before it was transferred to an airtight high-temperature stage (Japan High Tech Co., Ltd., 10042). Then, the high-temperature stage with the sampled salt was heated to 923 K under Ar atmosphere. Raman spectra were measured by a micro-Raman spectrometer (Tokyo Instruments, Nanofinder 30) using a laser source with an excitation wavelength of 532 nm. In addition to Raman spectroscopy, the sampled KF–KCl–WO_3 salt was also analyzed by X-ray diffractometry (XRD; Rigaku Ultima IV, Cu Kα, 40 kV, 40 mA).

Electrochemical measurements and galvanostatic electrolysis were performed using a three-electrode cell with an electrochemical measurement system (Hokuto Denko Corp., HZ-7000). The working electrodes were Cu foil (Nilaco Corp., 20 mm × 5 mm, thickness: 0.030 mm, 99.9%), Ag flag (Nilaco Corp., diameter: 2.0 mm,

*Electrochemical Society Member.
[a]Present address: Graduate School of Engineering, Kyoto University, Yoshida-honmachi, Sakyo-ku, Kyoto 606–8501, Japan.
[z]E-mail: nohira.toshiyuki.8r@kyoto-u.ac.jp

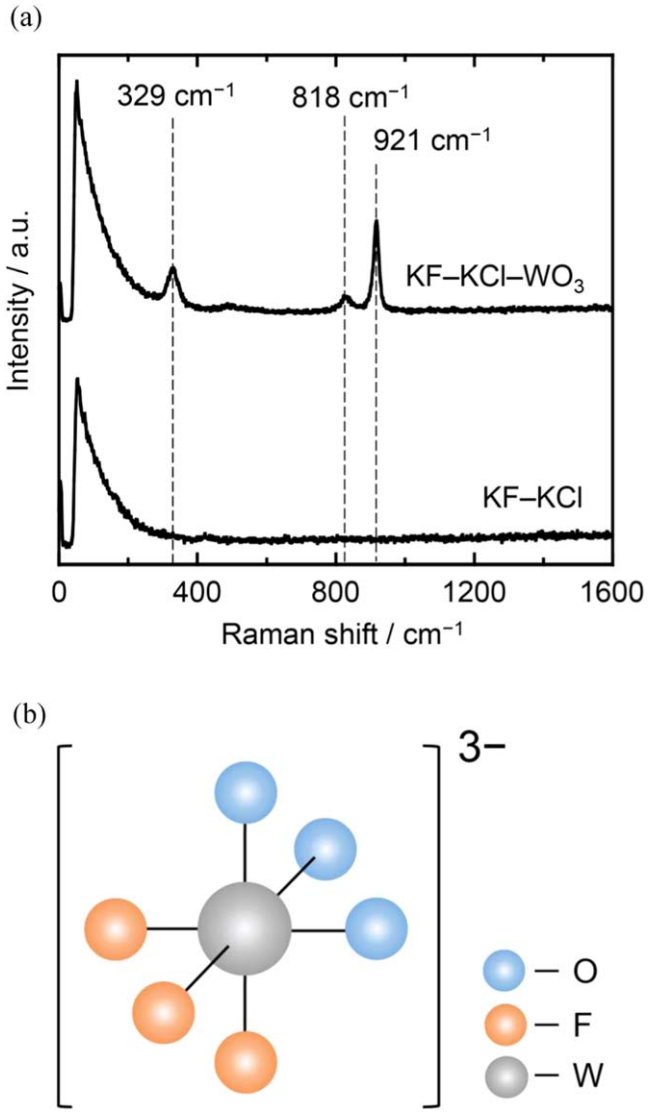

Figure 1. (a) Raman spectra of molten KF–KCl and molten KF–KCl–WO_3 (2.0 mol% added) at 923 K. (b) Structure of *fac*-$[WO_3F_3]^{3-}$ ion.

thickness: 0.1 mm, 99.98%), and Au flag (Nilaco Corp., diameter: 2.0 mm, thickness: 0.10 mm, 99.95%) electrodes. The structure of the flag electrodes was reported in our previous paper.[11] A glass-like carbon rod (Tokai Carbon Co., Ltd., diameter: 3.0 mm) was used as the counter electrode. A Pt wire (Nilaco Corp., diameter: 1.0 mm, 99.98%) was employed as the quasi-reference electrode. The potential of the quasi-reference electrode was calibrated with respect to the dynamic K^+/K or Cs^+/Cs potential determined by cyclic voltammetry at a Ag electrode. The melt temperature was measured using a type-K thermocouple. The electrolyzed samples on the Cu foils were soaked in distilled water for 60 min at 333 K to remove the salt adhered on the deposits.

Phase identification of the samples was conducted by using the same X-ray diffractometer described above. The surface and cross-sectional morphologies of the samples were observed using scanning electron microscopy (SEM; Keyence E8800). The samples were cut at the center and embedded in acrylic resin before cross-sectional SEM observation was performed. The samples were polished with emery papers and buffing compounds and then coated with Au using an ion-sputtering apparatus (Hitachi, Ltd., E-1010) to impart conductivity. The surface roughness (R_a: the arithmetic average roughness or S_a: the arithmetical mean height of the surface) of the

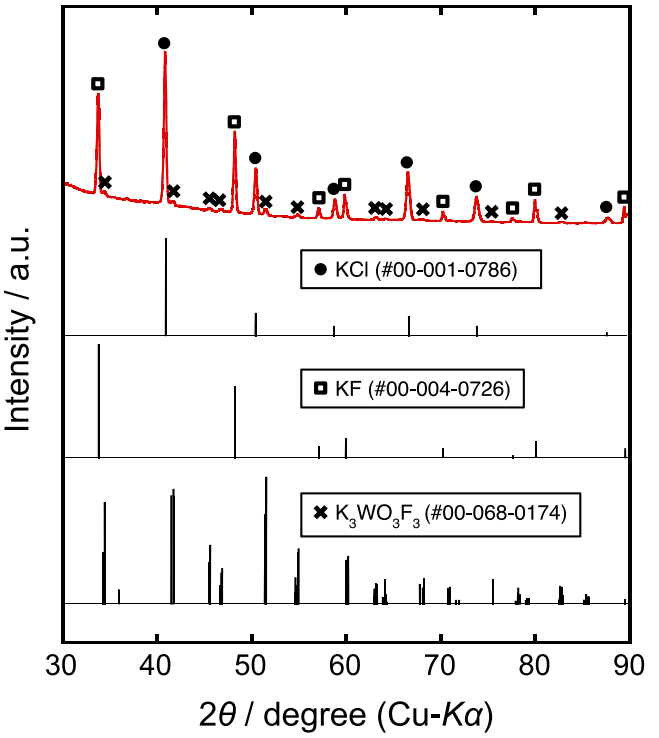

Figure 2. An XRD pattern of the solidified salt sampled from molten KF–KCl–WO_3 (2.0 mol% added) at 923 K.

samples was measured using a laser microscope (Keyence VK-X 1000).

Results and Discussion

KF–KCl–WO_3 melts.— *Raman and XRD analyses of the melts.*— Figure 1a shows the Raman spectrum of molten KF–KCl–WO_3 (2.0 mol% added) at 923 K along with the spectrum of mere molten KF–KCl for comparison. The molten KF–KCl–WO_3 exhibited three new bands at 329, 818, and 921 cm^{-1}. Krylov et al. reported the Raman bands for $K_3WO_3F_3$ crystals by quantum chemical calculations.[15] The wave numbers of the three new bands observed for molten KF–KCl–WO_3 are similar to those reported for $[WO_3F_3]^{3-}$ with *fac* conformation (Fig. 1a). Figure 1b shows the structure of the *fac*-$[WO_3F_3]^{3-}$ ion.

To confirm the existence of $K_3WO_3F_3$ in the melts, a small portion of the sampled salt was also analyzed by XRD at room temperature. In the obtained XRD pattern (Fig. 2), the characteristic pattern of $K_3WO_3F_3$ (PDF #00–068–0174) was clearly observed in addition to strong peaks of KCl and KF. It is also important to note that the observed crystal structure of $K_3WO_3F_3$ consists of *fac*-$[WO_3F_3]^{3-}$ ion.[16] According to both the Raman and XRD results, the dissolution state of WO_3 in the KF–KCl–WO_3 melt has been confirmed to be *fac*-$[WO_3F_3]^{3-}$ ions, hereafter referred as W(VI) ion for simplicity.

Cyclic voltammetry and XRD analysis.—Figure 3a shows the cyclic voltammogram at the Ag flag electrode both before and after the addition of WO_3 (2.0 mol%) in molten KF–KCl at 923 K. After the addition of WO_3, a cathodic current is observed from 1.65 V, which suggests the electrodeposition of W metal from W(VI) ions. After the reversal of the scan to positive direction, a considerable increase in the anodic current was observed from approximately 1.65 V, which is attributed to the anodic dissolution of the electrodeposited W metal. To confirm the anodic dissolution at more positive potential, cyclic voltammetry was performed at the Au flag electrode in molten KF–KCl–WO_3 (0.5 mol% added). Here, Au was

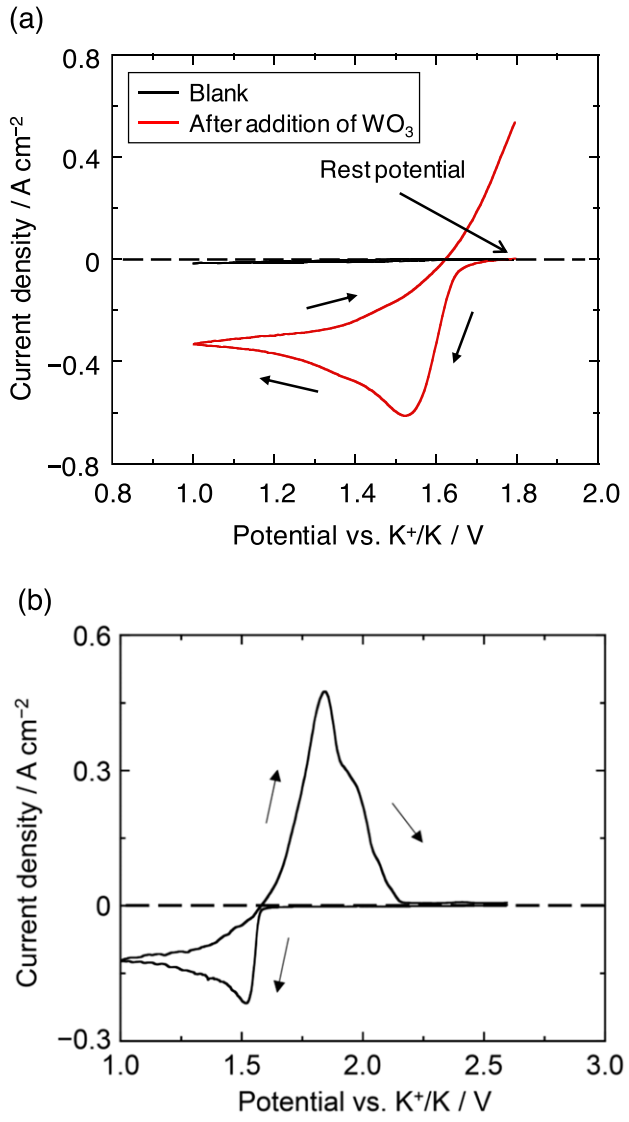

Figure 3. (a) Cyclic voltammogram at a Ag flag electrode in molten KF–KCl before and after addition of WO_3 (2.0 mol%) at 923 K. (b) Cyclic voltammogram measured in the wider potential region (1.0–2.6 V) at a Au flag electrode in molten KF–KCl–WO_3 (0.5 mol%) at 923 K. Scan rate: 0.5 V s^{-1}.

used because it has wider potential window in positive potential region compared with Ag. As shown in Fig. 3b, there is a clear anodic peak at 1.8 V, followed by a shoulder around 2.0 V. Although the anodic peak current density is larger than the cathodic peak current density, the sum of charges from cathodic currents during the forward and backward scans is roughly the same as the charges from anodic currents, giving a coulombic efficiency of 90%. However, the occurrence of a shoulder suggests that the anodic dissolution may proceed under the influence of multi-step reactions or kinetics. Although the anodic dissolution mechanism is of interest, it was not investigated further because the main purpose of the present study was cathodic electrodeposition.

A sample was prepared at a Cu foil electrode by galvanostatic electrolysis at 12.5 mA cm^{-2} for 120 min (charge density: 90 C cm^{-2}). The electrode potential maintained a stable value of ~1.56 V during the electrolysis. The optical images of the sample before and after the electrolysis demonstrated a change in its appearance from copper to bright gray (Fig. 4a). The XRD pattern of the sample after electrolysis clearly confirmed the electrodeposition of the α-W form of metallic W (Fig. 4b). Since the relative

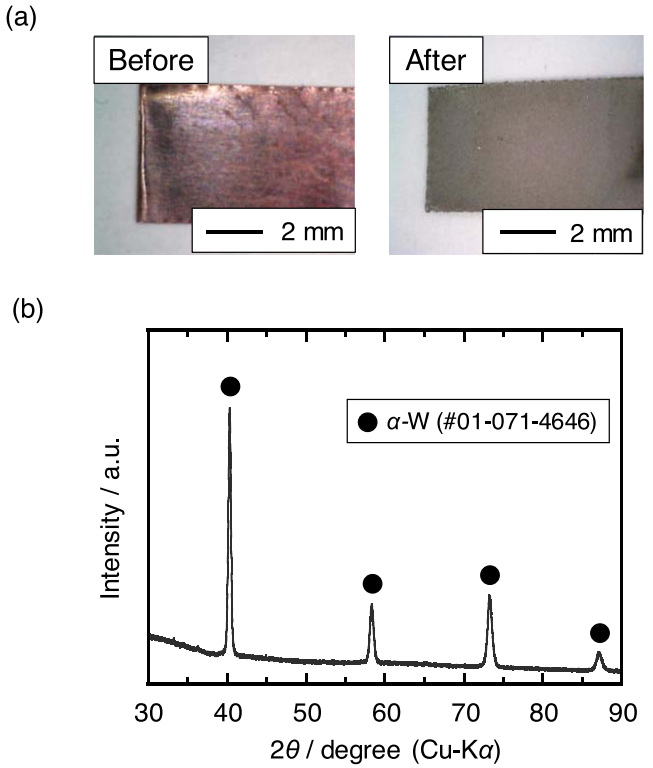

Figure 4. (a) Optical images of the sample before and after galvanostatic electrolysis of a Cu foil electrode at 12.5 mA cm^{-2} for 120 min in molten KF–KCl–WO_3 (2.0 mol% added) at 923 K. (b) An XRD pattern of the sample.

intensities for the observed pattern is similar to those for the reference powder pattern of W (PDF #01-071-4646), there is no distinct preferred orientation. The current efficiency based on the weight increase was calculated to be as high as 97%.

Effect of current density and W(VI) ion concentration.—To study the optimum electrodeposition conditions for obtaining both the dense and smooth W coatings, we conducted galvanostatic electrolysis at various current densities (12.5, 25, 50, and 100 mA cm^{-2}) and various amounts of WO_3 (0.50, 1.0, 1.5, and 2.0 mol%). During these experiments, the charge density was unified to 90 C cm^{-2} for accurate comparison. Figure 5 shows optical images of the samples after washing with distilled water. When higher current densities and lower W(VI) ion concentrations were employed, no (or negligible) amount of W deposits are observed, suggesting that either no W deposits were formed on the copper substrate or most of the deposited W were detached from the substrate during the water washing. The optical images of the samples obtained under such conditions are indicated by a yellow background in Fig. 5. In contrary, black or gray deposits were observed at lower current densities and higher W(VI) ion concentrations.

Figure 6 compares the SEM images of the samples obtained at various current densities and amounts of WO_3. Relatively smooth W coatings were deposited at lower current densities (12.5 and 25 mA cm^{-2}) and higher W(VI) ion concentrations (1.5 and 2.0 mol%), as indicated by the pale red backgrounds. The size of crystal grains of the deposited samples ranges from ~3 to 8 μm. In the cases of slightly larger current densities and slightly higher W(VI) ion concentrations, the W coatings exhibited rough surfaces that are indicated using the pale green backgrounds in Fig. 6.

Figure 7 shows the cross-sectional SEM images of the samples deposited on the Cu foil electrodes at different current densities and W(VI) ion concentrations. Dense W coatings with thicknesses of approximately 10–15 μm were observed for the samples at

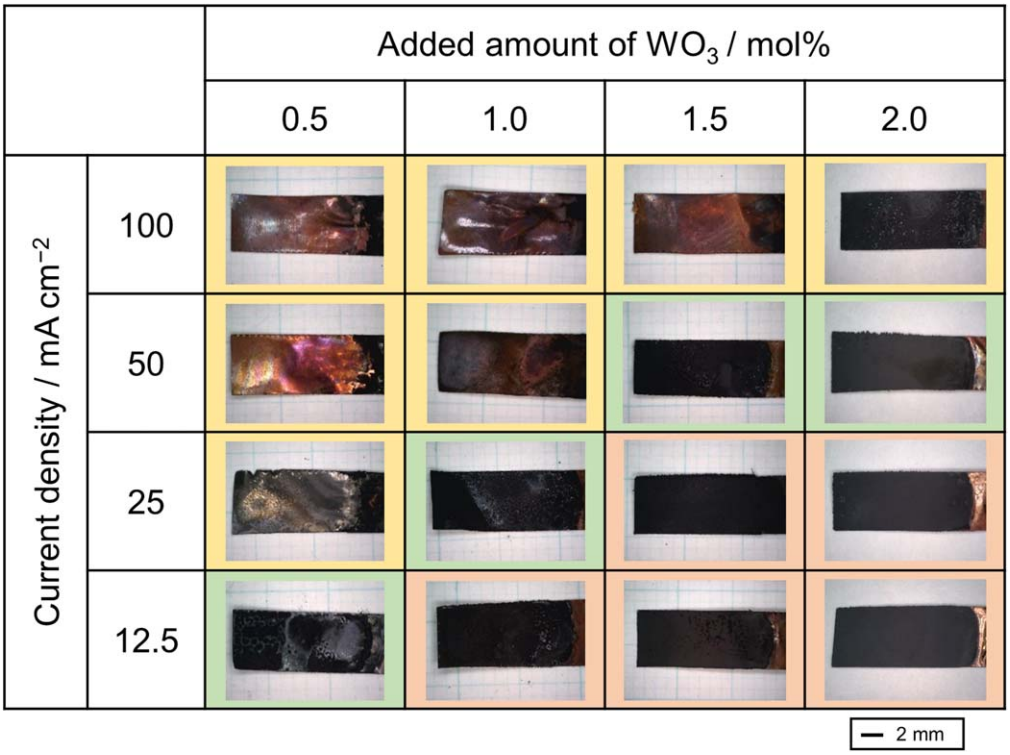

Figure 5. Optical images of the samples obtained by galvanostatic electrolysis of Cu foil electrodes at various current densities and added amounts of WO_3 in molten KF–KCl at 923 K. Charge density: 90 C cm^{-2}. The scale bar is common for all images.

lower current densities and higher W(VI) ion concentrations. The smoothest surface was confirmed for the sample prepared at a current density of 12.5 mA cm^{-2} and 2.0 mol% of WO_3. For this W coating, the arithmetic average roughness (R_a) was measured in several locations. The average R_a was calculated to be 1.02 ± 0.11 μm. In contrast, the W coatings with rougher surfaces were obtained in the conditions indicated by the pale green backgrounds in Fig. 7.

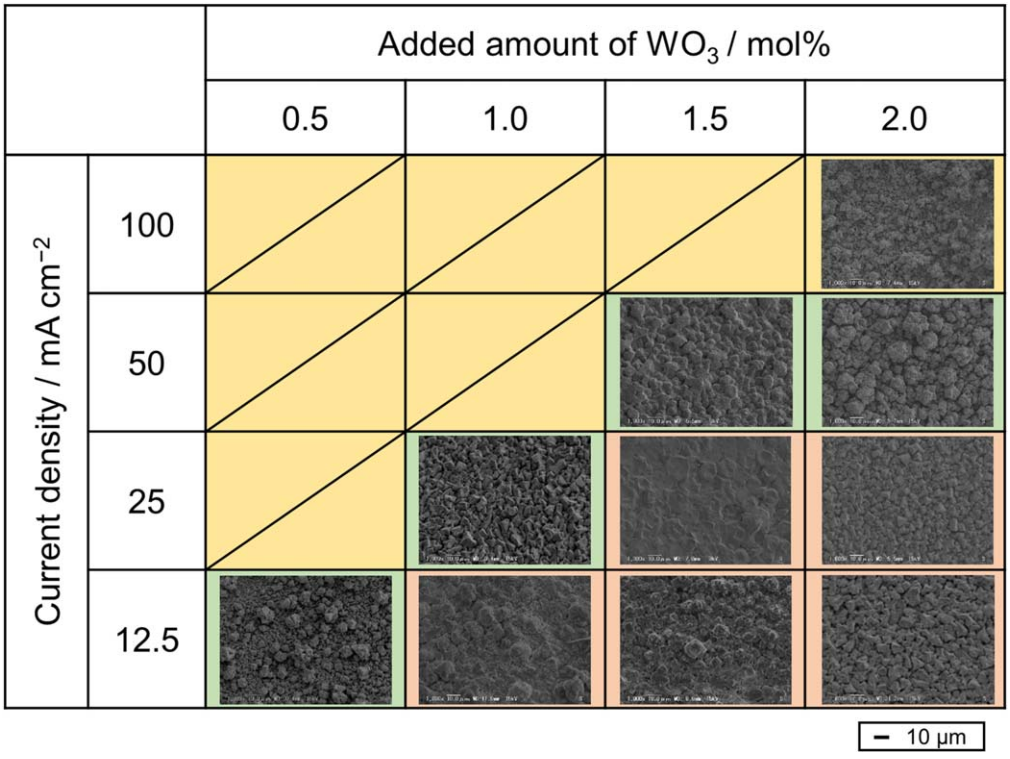

Figure 6. Surface SEM images of the samples obtained by galvanostatic electrolysis of Cu foil electrodes at various current densities and added amounts of WO_3 in molten KF–KCl at 923 K. Charge density: 90 C cm^{-2}. The scale bar is common for all images.

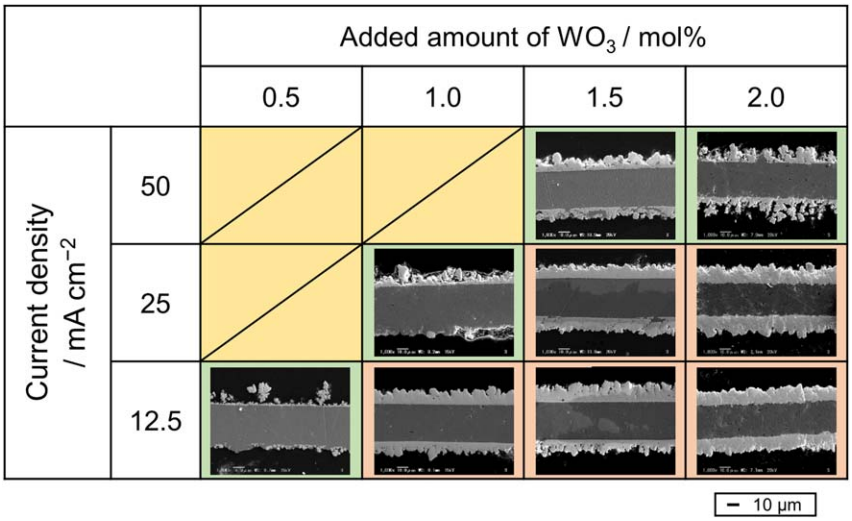

Figure 7. Cross-sectional SEM images of the samples obtained by galvanostatic electrolysis of Cu foil electrodes at various current densities and added amounts of WO_3 in molten KF–KCl at 923 K. Charge density: 90 C cm^{-2}. The scale bar is common for all images.

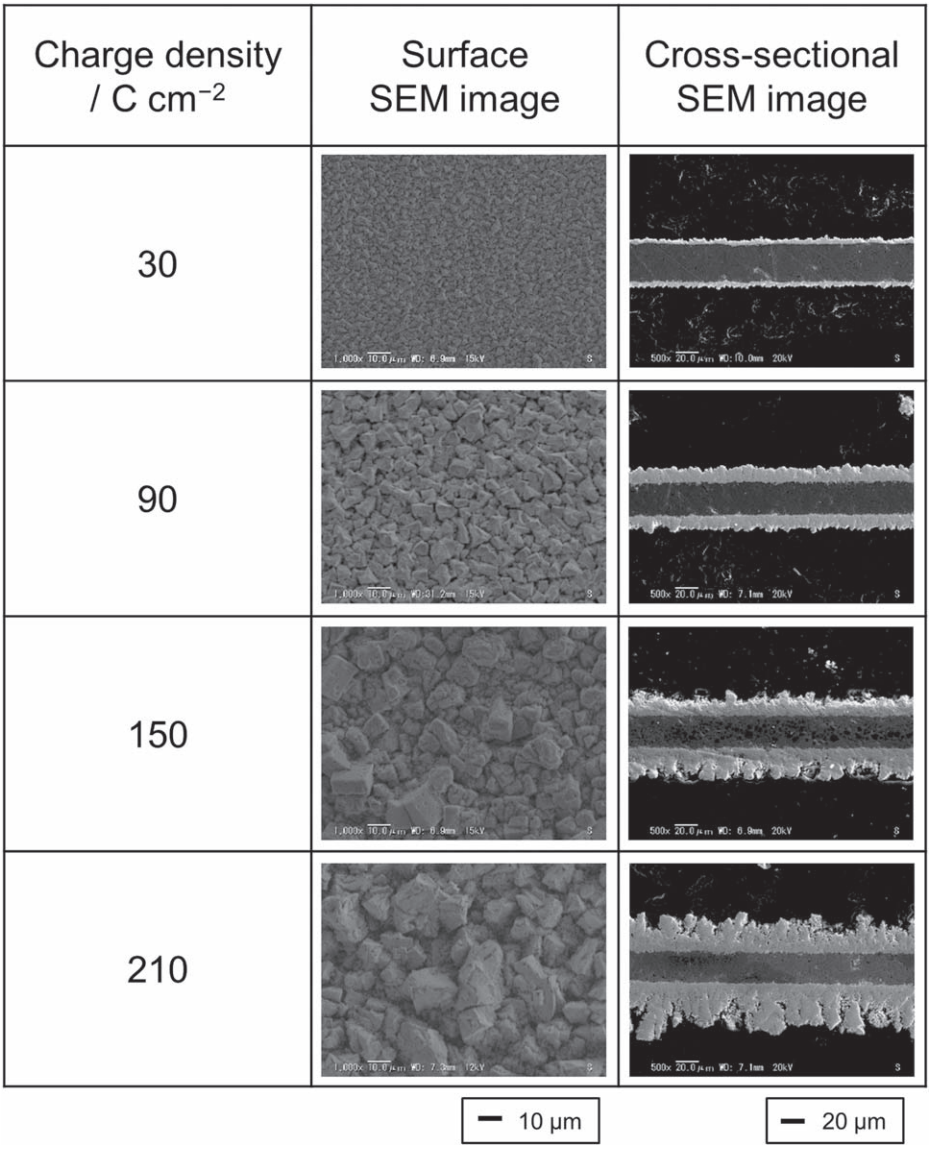

Figure 8. Surface and cross-sectional SEM images of the samples obtained by electrolysis of Cu foil electrodes at 12.5 mA cm^{-2} at various charge densities in molten KF–KCl–WO_3 (2.0 mol% added) at 923 K. The scale bar is common for all surface/cross-sectional images.

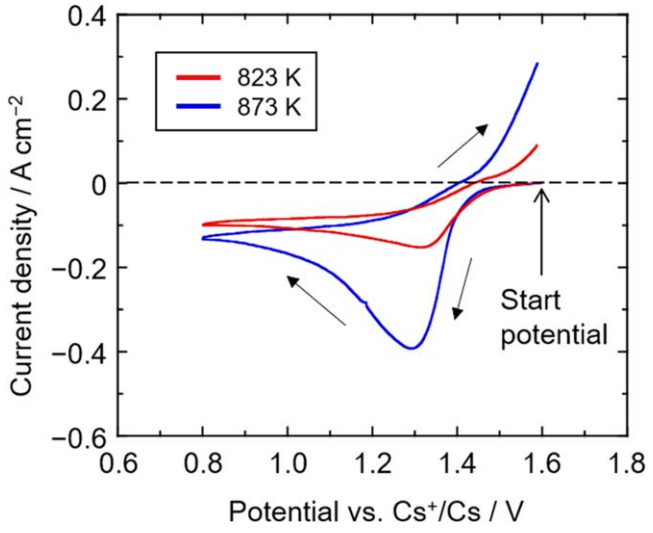

Figure 9. Cyclic voltammograms at a Au flag electrode in molten CsF–CsCl–WO_3 (2.0 mol% added) at 823 and 873 K. Scan rate: 0.5 V s^{-1}.

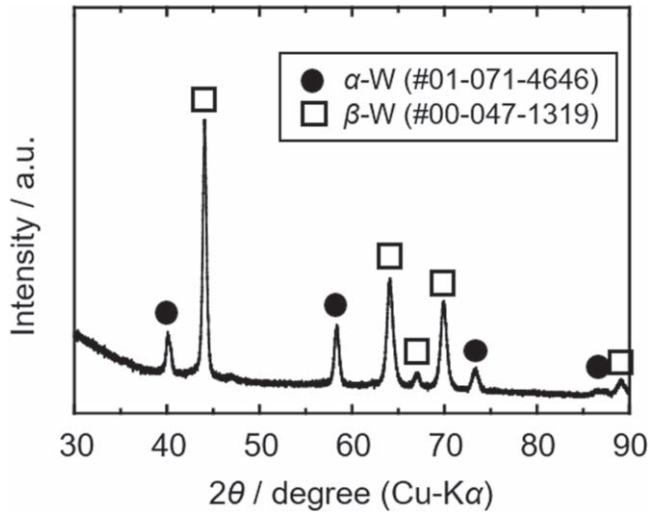

Figure 10. An XRD pattern of the sample obtained by galvanostatic electrolysis of a Cu foil electrode at 12.5 mA cm^{-2} for 120 min in molten CsF–CsCl–WO_3 (2.0 mol% added) at 873 K. Charge density: 90 C cm^{-2}.

Further, we aimed to prepare thicker W coatings using the above optimized conditions (12.5 mA cm^{-2} and 2.0 mol% WO_3), but with prolonged electrolysis time. Figure 8 shows the surface and cross-sectional SEM images of samples electrolyzed for 40, 120, 200 and 360 min; i.e., the time periods corresponding to the charge densities of 30, 90, 150 and 210 C cm^{-2}, respectively. The size of crystal grains increased with electrolysis time, as demonstrated by the surface SEM images. Although the coating thickness was successfully increased to ~30 μm at 210 C cm^{-2}, the surface roughness also increased significantly due to the larger crystal grains (Fig. 8).

CsF–CsCl–WO_3 melts.—In our previous study on the electrodeposition of Ti coatings in molten LiF–LiCl–Li_3TiF_6, the growth of crystal grains could be effectively suppressed and smoother deposits were obtained by lowering the temperature from 923 to 823 K.[17,18] Thus, in the present study, the temperature was reduced by utilizing CsF–CsCl eutectic melts with the aim to prepare smoother W coatings. Figure 9 shows cyclic voltammograms at a Au flag electrode in molten CsF–CsCl–WO_3 (2.0 mol% WO_3 added) at 823 and 873 K. As observed for the KF–KCl–WO_3 (2.0 mol% added) at 923 K, CsF–CsCl–WO_3 exhibited a cathodic current peak at approximately 1.3 V vs Cs^+/Cs at all temperatures, indicating the electrodeposition of W. However, the peak current density at 823 K was too small compared with 873 K. This result suggested that the solubility of WO_3 at 823 K was smaller than 2.0 mol%.

Figure 10 shows the XRD pattern of the sample prepared at a Cu foil electrode by galvanostatic electrolysis at 12.5 mA cm^{-2} for 120 min (charge density: 90 C cm^{-2}) and washed with water. Interestingly, XRD confirmed the existence of both α-W and β-W phases in the sample obtained in molten CsF–CsCl–WO_3. Among the observed α-W peaks, the strongest one was the 200 diffraction at 57.95 degree, which indicates the ⟨100⟩ preferred orientation. The codeposition of β-W might cause the preferred orientation for α-W. Concerning β-W, it is known to be the meta-stable phase of W with an A15 type crystal structure.[19] Recently, β-W has gained much attention because it exhibited the giant spin Hall effect.[19] The current efficiency based on the weight increase was calculated to be 94%.

Further, we aimed to prepare thicker W coatings by prolonging the electrolysis time to 360 min (charge density: 210 C cm^{-2}). Figure 11 shows the surface and cross-sectional SEM images of the samples obtained at 90 and 210 C cm^{-2} in molten CsF–CsCl–WO_3 (2.0 mol% added) at 873 K. As evident from the surface SEM, the sizes of crystal grains obtained in CsF–CsCl–WO_3 (2.0 mol% added) are considerably smaller than those formed in the KF–KCl–WO_3 (2.0 mol% added) at 923 K. The arithmetical mean height of the surface (S_a) was calculated for the W coatings obtained at 90 C cm^{-2} in molten CsF–CsCl–WO_3. Here we adopted S_a as a roughness parameter because it gives more significant value than *R*a. The obtained value is as small as 0.61 μm. Moreover, the cross-sectional SEM revealed that the thickness of W coating prepared in molten CsF–CsCl–WO_3 can be successfully increased to ~30 μm at 210 C cm^{-2} without any significant increase in the surface roughness.

Conclusions

The electrodeposition of W coatings was investigated at 923 K in KF–KCl eutectic melts containing 0.5–2.0 mol% of WO_3. Cathodic currents at a Ag electrode from 1.65 V vs K^+/K were interpreted as the electrodeposition of W metal from W(VI) ions. XRD analysis of the sample prepared at Cu foil confirmed the electrodeposition of α-W phase in molten KF–KCl–WO_3. Among various current densities (12.5–100 mA cm^{-2}) and amounts of WO_3 (0.5–2.0 mol%) investigated, 12.5 mA cm^{-2} and 2.0 mol% was found to be the optimum condition for obtaining better W coatings in molten KF–KCl–WO_3. The surface and cross-sectional SEM confirmed the formation of dense and smooth W coatings with a thickness of ~15 μm at the optimum condition. Although the thickness of the W coating in molten KF–KCl–WO_3 could be increased to ~30 μm by increasing the charge density to 210 C cm^{-2}, the surface roughness of the coating was significantly increased. In contrast, the galvanostatic electrolysis performed in molten CsF–CsCl–WO_3 (2.0 mol% added) at 12.5 mA cm^{-2} and 90 C cm^{-2} at 873 K resulted in better W coatings with smoother surfaces. The XRD analysis confirmed the presence of both α-W and β-W phases in the W coatings obtained in molten CsF–CsCl–WO_3. The SEM results of samples prepared in molten CsF–CsCl–WO_3 revealed the formation of both the dense and smooth W coatings with a thickness of ~30 μm at 12.5 mA cm^{-2} and 210 C cm^{-2}. Hence, the W coatings prepared in molten CsF–CsCl–WO_3 were both denser and smoother with controlled surface roughness than the coatings obtained in molten KF–KCl–WO_3 that exhibited an increase in the surface roughness along with their thickness.

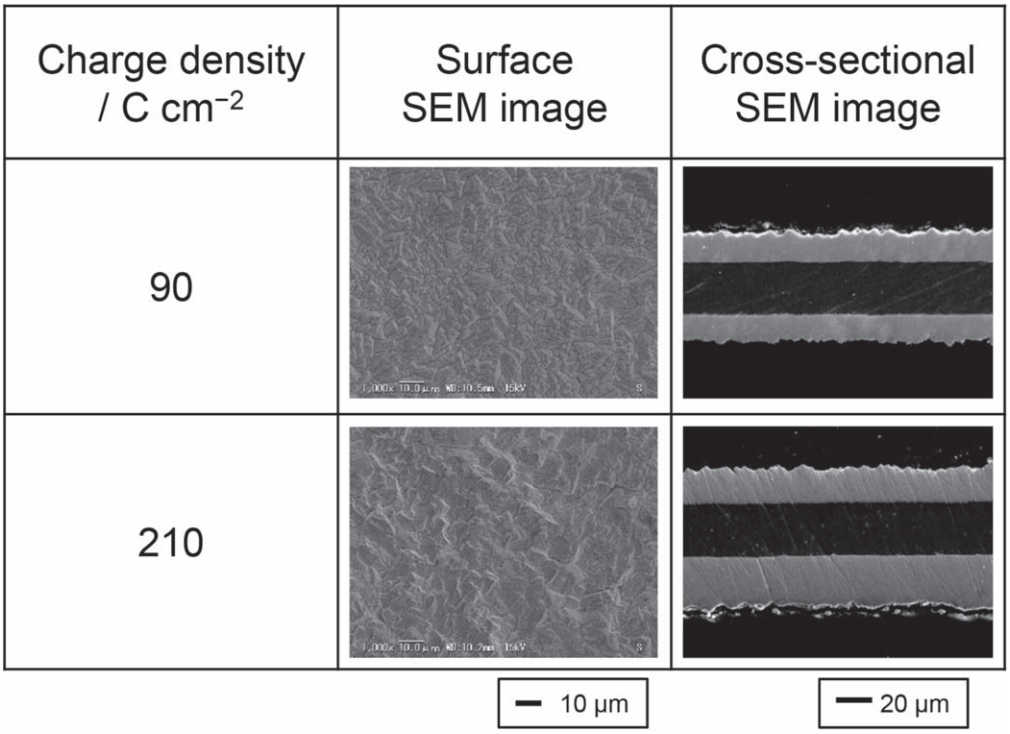

Figure 11. Surface and cross-sectional SEM images of the samples obtained by galvanostatic electrolysis of Cu foil electrodes at 12.5 mA cm^{-2} in molten CsF–CsCl–WO_3 (2.0 mol% added) at 873 K. Charge density: 90 and 210 C cm^{-2}.

Acknowledgments

A part of this study was conducted as collaborative research with Sumitomo Electric Industries, Ltd.

ORCID

Toshiyuki Nohira https://orcid.org/0000-0002-4053-554X
Xianduo Meng https://orcid.org/0000-0002-2450-6538
Yutaro Norikawa https://orcid.org/0000-0002-0861-5443
Kouji Yasuda https://orcid.org/0000-0001-5656-5359

References

1. S. Senderoff and G. Mellors, *Science*, **153**, 1475 (1966).
2. V. V. Malyshev, *Mater. Sci.*, **47**, 345 (2011).
3. K. H. Stern (ed.), *Metallurgical and Ceramic Protective Coatings* (Springer, Berlin: Dordrecht) Chap. 2, p. 31 (1996).
4. M. Masuda, H. Takenishi, and A. Katagiri, *J. Electrochem. Soc.*, **148**, C59 (2001).
5. J. Li, X. Zhang, Y. Liu, Y. Li, and R. Liu, *Rare Met.*, **32**, 512 (2013).
6. Y. Qi, Y. Tang, B. Wang, M. Zhang, X. Ren, Y. Li, and Y. Ma, *Int. J. Refract. Met. Hard Mater.*, **81**, 183 (2019).
7. V. A. Pavlovskii, *Inorg. Mater.*, **40**, 372 (2004).
8. V. A. Pavlovskii, *Inorg. Mater.*, **39**, 1208 (2004).
9. K. Koyama, M. Morishita, and T. Umezu, *Electrochemistry*, **67**, 667 (1999).
10. D. R. Lide (ed.), *CRC Handbook of Chemistry and Physics* (CRC Press, Boca Raton, FL) 88th ed., Chap. 4, p. 43 (2007).
11. K. Maeda, K. Yasuda, T. Nohira, R. Hagiwara, and T. Homma, *J. Electrochem. Soc.*, **162**, D444 (2015).
12. Y. Norikawa, K. Yasuda, and T. Nohira, *Mater. Trans.*, **58**, 390 (2017).
13. Y. Norikawa, K. Yasuda, and T. Nohira, *Electrochemistry*, **86**, 99 (2018).
14. Y. Norikawa, K. Yasuda, and T. Nohira, *J. Electrochem. Soc.*, **166**, D755 (2019).
15. A. S. Krylov, S. N. Sofronova, E. M. Kolensnikova, Y. N. Ivanov, A. A. Sukhovsky, S. V. Goryainov, A. A. Ivanenko, N. P. Shestakov, A. G. Kocharova, and A. N. Vtyurin, *J. Solid State Chem.*, **218**, 32 (2014).
16. M. S. Molokeev, S. V. Misyul, V. D. Fokina, A. G. Kocharova, and K. S. Aleksandrov, *Phys. Solid State*, **53**, 834 (2011).
17. Y. Norikawa, K. Yasuda, and T. Nohira, *J. Electrochem. Soc.*, **167**, 082502 (2020).
18. M. Unoki, Y. Norikawa, K. Yasuda, and T. Nohira, *ECS Trans.*, **98**, 393 (2020).
19. Q. Hao, W. Chen, and G. Xiao, *Appl. Phys. Lett.*, **106**, 182403 (2015).